This is a repository copy of *11β-hydroxysteroid dehydrogenase type 1 regulates glucocorticoid- induced insulin resistance in skeletal muscle*.

Article:

11β-Hydroxysteroid Dehydrogenase Type 1 Regulates Glucocorticoid-Induced Insulin Resistance in Skeletal Muscle

Stuart A. Morgan,[1] Mark Sherlock,[1] Laura L. Gathercole,[1] Gareth G. Lavery,[1] Carol Lenaghan,[2] Iwona J. Bujalska,[1] David Laber,[2] Alice Yu,[2] Gemma Convey,[2] Rachel Mayers,[2] Krisztina Hegyi,[3] Jaswinder K. Sethi,[3] Paul M. Stewart,[1] David M. Smith,[2] and Jeremy W. Tomlinson[1]

OBJECTIVE—Glucocorticoid excess is characterized by increased adiposity, skeletal myopathy, and insulin resistance, but the precise molecular mechanisms are unknown. Within skeletal muscle, 11β-hydroxysteroid dehydrogenase type 1 (11β-HSD1) converts cortisone (11-dehydrocorticosterone in rodents) to active cortisol (corticosterone in rodents). We aimed to determine the mechanisms underpinning glucocorticoid-induced insulin resistance in skeletal muscle and indentify how 11β-HSD1 inhibitors improve insulin sensitivity.

RESEARCH DESIGN AND METHODS—Rodent and human cell cultures, whole-tissue explants, and animal models were used to determine the impact of glucocorticoids and selective 11β-HSD1 inhibition upon insulin signaling and action.

RESULTS—Dexamethasone decreased insulin-stimulated glucose uptake, decreased IRS1 mRNA and protein expression, and increased inactivating pSer^{307} insulin receptor substrate (IRS)-1. 11β-HSD1 activity and expression were observed in human and rodent myotubes and muscle explants. Activity was predominantly oxo-reductase, generating active glucocorticoid. A1 (selective 11β-HSD1 inhibitor) abolished enzyme activity and blocked the increase in pSer^{307} IRS1 and reduction in total IRS1 protein after treatment with 11DHC but not corticosterone. In C57Bl6/J mice, the selective 11β-HSD1 inhibitor, A2, decreased fasting blood glucose levels and improved insulin sensitivity. In KK mice treated with A2, skeletal muscle pSer^{307} IRS1 decreased and pThr^{308} Akt/PKB increased. In addition, A2 decreased both lipogenic and lipolytic gene expression.

CONCLUSIONS—Prereceptor facilitation of glucocorticoid action via 11β-HSD1 increases pSer^{307} IRS1 and may be crucial in mediating insulin resistance in skeletal muscle. Selective 11β-HSD1 inhibition decreases pSer^{307} IRS1, increases pThr^{308} Akt/PKB, and decreases lipogenic and lipolytic gene expression that may represent an important mechanism underpinning their insulin-sensitizing action. *Diabetes* 58:2506–2515, 2009

The costs of publication of this article were defrayed in part by the payment of page charges. This article must therefore be hereby marked "advertisement" in accordance with 18 U.S.C. Section 1734 solely to indicate this fact.

The pathophysiological effects of glucocorticoids are well described and impact upon almost all organ systems within the body. This is highlighted in patients with glucocorticoids excess, Cushing's syndrome characterized by central obesity, hypertension, proximal myopathy, insulin resistance, and in some cases overt type 2 diabetes. In addition, up to 2.5% of the population are taking prescribed glucocorticoids (1), and their side effects represent a considerable clinical burden for both patient and clinician.

Glucocorticoids induce whole-body insulin resistance (2); however, the precise molecular mechanisms that underpin this observation have not been defined in detail. In simple obesity and insulin resistance, circulating cortisol levels are not elevated (3), but in key insulin target tissues including liver, fat, and muscle, glucocorticoid availability to bind and activate the glucocorticoid receptor is controlled by 11β-hydroxysteroid dehydrogenase type 1 (11β-HSD1). 11β-HSD1 is an endo-lumenal enzyme that interconverts inactive (cortisone in humans and 11-dehydrocorticosterone [11DHC] in rodents) and active glucocorticoids (cortisol in humans and corticosterone [CORT] in rodents) (4). Critically, the directionality of 11β-HSD1 activity is cofactor (NADPH) dependent that is supplied by a tightly associated endo-lumenal enzyme, hexose-6-phopshate dehydrogenase (H6PDH). Decreases in H6PDH expression and activity decrease 11β-HSD1 oxo-reductase and increase dehydrogenase activity (5). Despite this bidirectional potential, the predominant direction of activity in liver, adipose, and muscle is oxo-reductase generating active glucocorticoid (cortisol and CORT), therefore, amplifying local glucocorticoid action.

Binding of insulin to its cell surface receptor leads to a conformational change and tyrosine autophosphorylation. Consequently, the insulin receptor substrate (IRS) family of adaptor proteins are recruited to the intracellular domain of the receptor and are phosphorylated at multiple tyrosine residues by the receptor tyrosine kinase to permit the docking of phosphatidylinositol-3-kinase (PI3K) and subsequent generation of PI(3,4,5)P$_3$. Generation of this second messenger acts to recruit the Akt/PKB family of serine/threonine kinases to the plasma membrane where they are then activated (6). Further downstream, activated Akt1/protein kinase B (PKB) phosphorylates a rab-GAP (GTPase) protein, AS160, which is a crucial regulator of the translocation of GLUT4 GLUT storage vesicles to the plasma membrane (7). It is this mechanism that permits

insulin-stimulated glucose entry into target tissues including skeletal muscle (8).

The molecular mechanisms underpinning insulin resistance are complex and variable. Serine/threonine phosphorylation of IRS1 (in particular Ser[307] phosphorylation) has been shown to negatively regulate insulin signaling through multiple mechanisms including decreased affinity for the insulin receptor and increased degradation (9,10).

The interaction of glucocorticoids and the insulin signaling cascade has only been examined in a small number of studies that have offered variable explanations for the induction of insulin resistance (11–14). Importantly, the role of serine phosphorylation and the impact of prereceptor glucocorticoid metabolism have not been explored. The 11β-HSD1 knockout mouse is relatively insulin sensitive (15), and specific inhibitors of 11β-HSD1 improve lipid profiles, glucose tolerance, and insulin sensitivity and have considerable potential as therapeutic agents (16–18). However, the molecular mechanisms that underpin these observations remain to be defined.

Therefore, we have characterized the impact of glucocorticoids upon the insulin-signaling cascade and analyzed the expression, activity, and functional impact of 11β-HSD1 in vitro and using in vivo mouse models.

RESEARCH DESIGN AND METHODS

Cell culture. Mouse skeletal muscle cell line, C2C12 myoblasts (ECACC, U.K.), were grown in DMEM (PAA, U.K.) supplemented with 10% FBS (37°C, 5% CO_2). Cells were grown to 60–70% confluence before differentiation (initiated by replacing growth media with DMEM with 5% horse serum). After 8 days, myoblasts had fused to form multinucleated myotubes. Before treatment, cells were washed out with serum-free media for 4 h. For experiments examining Ser[24] phosphorylation, C2C12 cells stably overexpressing myc-rIRS1 were generated and used as described previously for 3T3-L1 adipocytes (19).

Primary human myoblasts were obtained from PromoCell (Heidelberg, Germany). Myoblasts were cultured to confluence, as per the manufacturer's guidelines using the supplied media. Once confluent, media was changed to a chemically defined media (PromoCell, Germany) including 2% horse serum and cells differentiated into myotubes for 11 days. After differentiation, cells were incubated with serum-free media for 4 h before treatment.

Unless otherwise stated, for all cell culture experiments investigating insulin-signaling cascade protein phosphorylation, media was spiked with human insulin (0.1 µg/ml, Sigma, U.K.) for the final 15 min of the treatment period to achieve insulin stimulation. In experiments using the glucocorticoid receptor antagonist, RU38486, cells were pretreated with RU38486 (10 µmol/l) for 10 min before adding Dexamethasone (Dex). Treatments and reagents were supplied by Sigma, Poole, U.K. unless otherwise stated. Selective 11β-HSD1 inhibitors (A1 and A2, >95% and >99% purity, respectively) were provided through material transfer agreements with AstraZeneca (Macclesfield, U.K.). Inhibitor properties are presented within the results section.

RNA extraction, reverse transcription PCR, and real-time PCR. Total RNA was extracted from cell lysates using the Tri-Reagent system and from whole-tissue explants using RNeasy Fibrous Tissue Mini Kit (Qiagen). Integrity, concentration, and reverse transcription were performed as we have previously described (20). Specific mRNA levels were determined using an ABI 7500 sequence detection system (Perkin-Elmer Applied Biosystems, Warrington, U.K.). Reactions were performed in 20 µl volumes on 96-well plates in reaction buffer containing $2 \times$ TaqMan Universal PCR Master mix (Applied Biosystems, Foster City, CA). Probes and primers for all genes were supplied by applied biosystems 'assay on demand' (Applied Biosystems). All reactions were normalized against 18S rRNA as an internal housekeeping gene.

Data were obtained as ct values (ct = cycle number at which logarithmic PCR plots cross a calculated threshold line) and used to determine Δct values with Δct = (ct of the target gene) – (ct of the housekeeping gene). Data are expressed as arbitrary units using the following transformation (expression = $10^5 \times [2^{-\Delta ct}]$ arbitrary units [AUs]). When used, fold changes were calculated using the following equation: [fold increase = $2^{-\text{difference in } \Delta ct}$].

Genecard analysis. Taqman 348-well custom arrays were purchased from Applied Biosystems containing 45 custom genes and 3 housekeeping genes. Five hundred nanograms of cDNA were mixed with Taqman universal PCR

master mix (Applied Biosystems), and the array was run on an ABI 7900HT Fast Real-Time PCR System (Applied Biosystems). Data were obtained as ct values and fold changes calculated. Results were validated with standard Taqman RT-PCR.

Protein extraction and immunoblotting. Cells were scraped into 100 µl RIPA buffer (50 mmol/l Tris pH 7.4, 1% NP40, 0.25% sodium deoxycholate, 150 mmol/l NaCl, 1 mmol/l EDTA), 1 mmol/l phenylmethylsulfonyl fluoride, and protease inhibitor cocktail (Roche, Lewes, U.K.), incubated at −80°C (10 min) on ice (30 min), and centrifuged at 4°C (10 min, 14,000 rpm). The supernatant was transferred to a fresh tube and total protein concentration determined by a commercially available assay (Bio-Rad Laboratories, Hercules, CA).

Twenty micrograms of protein was resolved on an SDS-PAGE gel (acrylamide percentage varied according to protein size). Proteins were transferred onto nitrocellulose membrane, Hybond ECL (GE Healthcare, Chalfont St. Giles, U.K.). Primary (anti-IRS1, anti-pSer[307] IRS1, anti-IRS2, and anti-AS160 from Upstate, Dundee, U.K.; anti-PKB/akt, anti-pSer[473] PKB/akt [recognizing isoforms 1 and 2], and anti-Thr[308] Akt/PKB from R&D Systems, Abingdon, U.K.; and anti-pTyr[608] IRS1 from Biosource, Nivelles, Belgium) and secondary antibodies (Dako, Glostrop, U.K.) were used at a dilution of 1/5,000. Membranes were reprobed for β-actin and primary and secondary antibodies used at a dilution of 1/5,000 (Abcam plc, Cambridge, U.K.). Bands were visualized using ECL detection kit (GE Healthcare, Chalfont St. Giles, U.K.) and quantified with Genesnap by Syngene (Cambridge, U.K.).

Glucose transport assay. Glucose uptake activity was analyzed by measuring the uptake of 2-deoxy-D-[³H] glucose as described previously (21). After treatment, cells were washed three times with Krebs-Ringer-Hepes (KRP) buffer and incubated with 0.9 ml KRP buffer at 37°C for 20 min. Insulin (0.5 µg/ml) was then added, and the cells were incubated at 37°C for 20 min. Glucose uptake was initiated by the addition of 0.1 ml KRP buffer and 37MBq/l 2-deoxy-D-[³H] glucose (GE Healthcare) and 7 mmol/l glucose as final concentrations. After 60 min, glucose uptake was terminated by washing the cells three times with cold PBS. Cells were lysed and radioactivity retained by the cell lysates determined by scintillation counting.

11β-HSD1 assay. Briefly, intact cells were incubated with 100 nmol/l 11DHC and tritiated tracer for 2–24 h dependent upon assay system. In studies using selective 11β-HSD1 inhibitors, cells were incubated for 24 h with inhibitor before 11β-HSD1 assay being performed. Steroids were then extracted using dichloromethane, separated using a mobile phase consisting of ethanol and chloroform (8:92) by thin layer chromatography, and scanned using a Bioscan 3000 image analyzer (Lablogic, U.K.). Protein levels were assayed using a commercially available kit (Bio-Rad, Richmond, CA).

Mouse protocols. The selective 11β-HSD1 inhibitor A2 was used in two separate mouse protocols. All experimental procedures were conducted in accordance with the Animal Scientific Procedures Act 1986, Animal Welfare Act 2006, and local guidelines. First, male C57Bl6/J mice (6 weeks of age) were maintained for 20 weeks on a diet comprising 48 kcal% fat/10 kcal% fructose (Research Diets RD06072801, New Brunswick, NJ). Mice were housed with a standard light cycle (06:00 h on/18:00 h off), and A2 was administered (20 mg/kg b.i.d) by oral gavage for 28 days and compared against vehicle-control and pair-fed, vehicle-treated animals ($n = 9$–10). Food intake was assessed over the 28-day period, and on day 24 after 12-h fast, an oral glucose tolerance test (OGTT, 2 g/kg) was performed. Conscious tail-prick samples were analyzed for glucose using the Accu-Chek Aviva system (Roche) and for insulin using Ultra Sensitive Mouse Insulin ELISA kits (Crystal Chem #90800, Downers Grove, IL).

Separately, the impact of A2 upon skeletal muscle gene and protein expression in an additional hyperglycemic model were determined (male KK/Ta Jcl mice aged 7 weeks; CLEA Japan, Tokyo, Japan). Animals had free access to water and irradiated RM3 (E) diet composed of 11.5 kcal% fat, 27 kcal% protein, and 62 kcal% carbohydrate (Special Diets Services, Witham, U.K.). Compound A2 (20 mg/kg) or vehicle (10 ml/kg) was administered by oral gavage at 08:00 and 20:00 h for 4 consecutive days. After the administration of the third dose of A2, mice were anesthetized by inhalation of 2–3% v/v isoflurane (vaporized by oxygen at 1.6 l/min flow rate) and a 5 mg slow-release cortisone pellet ($\sim$8 mg $\cdot$ kg^{-1} $\cdot$ day^{-1} in a 29 g mouse) implanted subcutaneously in the lateral aspect of the neck (Innovative Research of America, Sarasota, FL). On day 4, 1–2 h after the seventh oral dose of A2, a rising-dose carbon dioxide concentration was used to humanely kill mice in the fed state and femoral quadriceps muscles were removed and snap frozen in liquid nitrogen.

Statistical analysis. Where data were normally distributed, unpaired Student's t tests were used to compare single treatments to control. If normality tests failed, then nonparametric tests were used. One-way ANOVA on ranks was used to compare multiple treatments, doses, or times (SigmaStat 3.1; Systat Software, Point Richmond, CA). Statistical analysis on real-time PCR data was performed on mean Δct values.

TABLE 1
mRNA expression of key components of the insulin-signaling cascade and glucocorticoid metabolism in C2C12 rodent skeletal myocytes measured using real-time PCR after treatment with Dex (1 μmol/l, 24 h) with or without the glucocorticoid receptor antagonist, RU38486 (10 μmol/l)

Gene	Control	Dexamethasone (1 μmol/l, 24 h)	Dexamethasone (1 μmol/l, 24 h) + RU38486 (10 μmol/l, 24 h)
InsR	4.4 ± 0.4	6.1 ± 0.5†	5.4 ± 0.5
IRS1	8.7 ± 0.7	4.5 ± 0.4*	7.5 ± 0.7§
AKT1	45.2 ± 5.4	39.4 ± 2.8	45.1 ± 3.4
AKT2	1.5 ± 0.3	2.3 ± 0.1*	1.9 ± 0.3
PI3K(p85)	1.4 ± 0.2	2.2 ± 0.2*	2.2 ± 0.1
GLUT4	2.3 ± 0.3	13.1 ± 1.5‡	3.7 ± 0.4∥
11βHSD1	32.9 ± 2.9	27.6 ± 2.7	35.6 ± 3.6
H6PDH	0.10 ± 0.0149	1.30 ± 0.07‡	0.18 ± 0.02¶
AS160	0.12 ± 0.02	0.23 ± 0.02*	0.12 ± 0.01§

Data are the mean values from $n = 5$ experiments and expressed as AUs ± SE (*$P < 0.05$, †$P < 0.01$, and ‡$P < 0.001$ vs. control; §$P < 0.05$, ∥$P < 0.01$, and ¶$P < 0.001$ vs. Dex).

RESULTS

Glucocorticoid impact upon the insulin-signaling cascade. In agreement with published data, treatment with the synthetic glucocorticoid Dex (1 μmol/l, 24 h) decreased insulin-stimulated glucose uptake (2.1 ± 0.3 vs. 1.7 ± 0.2 dpm × 10^5, $P < 0.05$, $n = 4$) consistent with the induction of insulin resistance in differentiated rodent C2C12 skeletal myocytes.

Using real-time PCR, Dex (1 μmol/l, 24 h) decreased mRNA expression of IRS1 (8.7 ± 0.7 vs. 4.5 ± 0.4 AU, $P < 0.05$, $n = 5$), an effect that was blocked by the glucocorticoid antagonist RU-38486 (Table 1). In contrast, IR, Akt/PKB2, PI3K, AS160, and GLUT4 expression all increased after Dex treatment. RU38486 reversed only the effects of Dex upon GLUT4 and AS160 expression. Although Dex treatment did not alter 11β-HSD1 expression, H6PDH expression increased (0.10 ± 0.01 vs. 1.30 ± 0.07 AU, $P < 0.001$) and was reversed by coincubation with RU38486 (0.18 ± 0.02 AU, $P < 0.001$ vs. Dex). Absolute mRNA expression data after Dex treatment with and without the glucocorticoid receptor antagonist RU38486 are presented in Table 1.

At the protein level, treatment with Dex decreased IRS1 total protein expression (0.4-fold, $P < 0.05$) that was recovered by coincubation with RU38486 (Fig. 1A and B). Insulin-stimulated, activating Tyr^{608} phosphorylation of IRS1 was unchanged with Dex treatment (Fig. 1A and B). However, we observed enhanced inactivating Ser^{307} phosphorylation (3.3-fold, $P < 0.05$) after Dex treatment that was prevented by RU-38486 (Fig. 1A and B). Total IRS2 protein expression was increased by Dex (1.7-fold, $P < 0.001$) (Fig. 1A and C). Further downstream, Akt/PKB protein expression did not change with Dex treatment, but activating Ser^{473} phosphorylation decreased (0.5-fold, $P < 0.05$) (Fig. 1A and D). Dex treatment increased AS160 expression 1.5-fold ($P < 0.05$), which was blocked by coincubation with RU38486 (Fig. 1A and E).

Diacylglycerol (DAG)-dependent protein kinase C (PKC) isoforms have been implicated in the phosphorylation of IRS1 at Ser^{24}, and this has been linked to the pathogenesis of insulin resistance (19). We examined the effect of Dex using C2C12 cells stably overexpressing IRS1. Although Dex increased Ser^{307} phosphorylation in this model, there was no detectable impact upon Ser^{24} phosphorylation or ectopic IRS1-myc protein levels (Fig. 1F).

To determine whether our observations with synthetic glucocorticoids were applicable in a physiological context, further experiments were performed using endogenous rodent glucocorticoids (11DHC and CORT). Consistent with our observations using Dex, CORT caused a dose- and time-dependent decrease in IRS1 total protein expression (dose: 1.0 [control] vs. 0.59-fold [100 nmol/l], $P < 0.01$, 0.47-fold [250 nmol/l], $P < 0.05$, 0.44-fold [500 nmol/l], $P < 0.01$, 0.38-fold [1,000 nmol/l], $P < 0.01$; time: 1.0 [control] vs. 0.19 ± 0.04 [48 h], $P < 0.05$) (Fig. 2A and B). This was accompanied by a dose- (1.0 [control] vs. 2.80-fold [250 nmol/l], $P < 0.01$, 3.99-fold [500 nmol/l], $P < 0.01$, 4.37-fold [1,000 nmol/l], $P < 0.001$) (Fig. 2A) and time- (1.0 [control] vs. 3.0 ± 0.08 [48 h], $P < 0.05$) (Fig. 2B) dependent increase in Ser^{307} phosphorylation.

11β-HSD1 in rodent and human skeletal muscle. 11β-HSD1 mRNA was highly expressed in C2C12 cells. Expression was also detected in whole-tissue explants of mouse quadriceps muscle, although levels were lower than those seen in liver and adipose tissue (Table 2). In all systems (C2C12 cells, human primary cultures, and whole-tissue explants from mice), functional, bidirectional 11β-HSD1 activity was demonstrated with predominant oxo-reductase activity (Fig. 3A and B). In mouse quadriceps explants, oxo-reductase activity was significantly decreased after coincubation with the nonselective 11β-HSD inhibitor, glycyrrhetinic acid (2 μmol/l, 2 h) (114.0 ± 5.7 vs. 44.6 ± 11.1 pmol · g^{-1} · h^{-1}, $P < 0.05$) (Fig. 3A and B). A1 and A2 are selective 11β-HSD1 inhibitors provided through an investigator-led collaboration with AstraZeneca. A1 has a half-maximal inhibitory concentration (IC$_{50}$) for human recombinant 11β-HSD1 of 0.3 nmol/l and for rat 637 nmol/l, mouse 33 nmol/l, and human 11β-HSD2 >15 μmol/l. A2 has an IC$_{50}$ for human recombinant 11β-HSD1 of 7 nmol/l and for rat 94 nmol/l, mouse 26 nmol/l, and human 11β-HSD2 >15 μmol/l. Treatment with A1 (1 μmol/l, 24 h), significantly decreased oxo-reductase activity in mouse quadriceps whole-tissue explants, differentiated C2C12 cells, and primary cultures of differentiated human skeletal myocytes (Fig. 3C).

Functional impact of 11β-HSD1 inhibition
Rodent and human cell lines and primary cultures. Paralleling our observations with Dex and CORT, 11DHC (250 nmol/l, 24 h) decreased IRS1 total protein expression (0.5-fold, $P < 0.05$) and increased pSer^{307} IRS1 (2.0-fold, $P < 0.05$) in C2C12 cells. Coincubation with the nonselective 11β-HSD inhibitor glycyrrhetinic acid (2.5 μmol/l, 24 h) reversed 11DHC-induced pSer^{307} IRS1 to levels seen in control untreated cells (1.1-fold, $P = 0.56$ vs. control) (Fig. 4A). Glycyrrhetinic acid treatment alone was without effect (data not shown). Similarly, observations with the selective 11β-HSD1 inhibitor A1 (2.5 μmol/l, 24 h) mirrored those with glycyrrhetinic acid, completely blocking the effects of 11DHC to decrease total IRS1 expression and increase pSer^{307} IRS1 (Fig. 4B). Extending these findings, in primary cultures of human skeletal muscle, cortisone (250 nmol/l, 24 h) decreased insulin-stimulated pThr^{308} Akt/PKB without altering total Akt/PKB protein expression. These observations were completely abolished following coincubation with A1 (Fig. 4C).
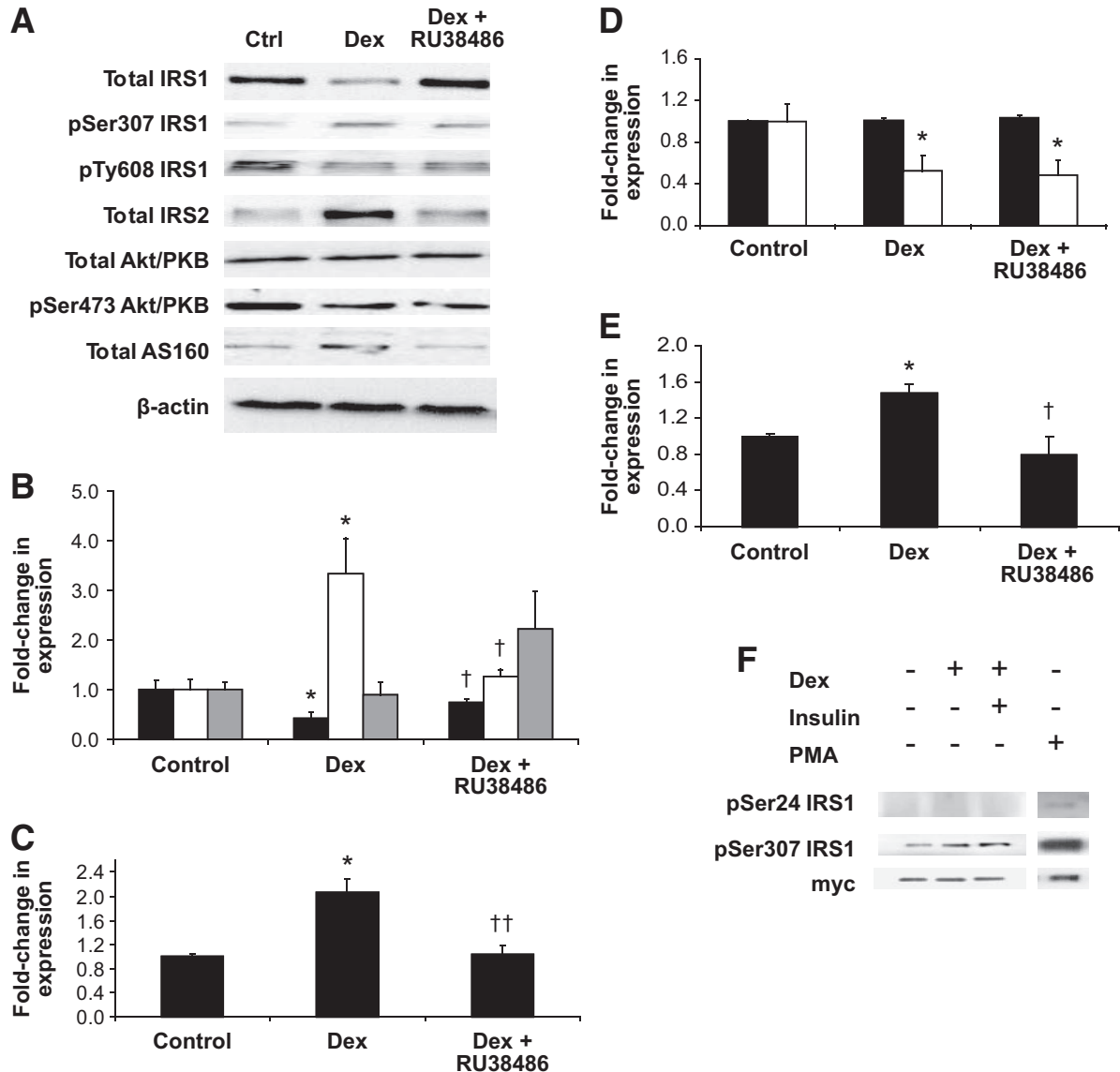
FIG. 1. Dex treatment (1 μmol/l, 24 h) in C2C12 rodent skeletal myocytes decreases IRS1 total protein expression, increases pSer[307] IRS1, but does not change pTyr[608] IRS1. These observations are reversed by coincubation with the glucocorticoid antagonist RU38486. IRS2 expression increased after Dex treatment. Although Akt/PKB expression does not change, activating pSer[473] Akt/PKB decreases but is not recovered by coincubation with RU38486. Total AS160 protein expression increased after Dex pretreatment and was reversed with RU38486. Representative Western blots are shown in panel 1*A* with quantitation relative to β-actin as internal loading control shown in subsequent panels (IRS1 [total IRS1: black bars, pSer[307] IRS1: white bars, pTyr[608] IRS1: gray bars] [*B*], IRS2 [*C*], akt/PKB [total Akt/PKB: black bars, pSer[473] Akt/PKB: white bars] [*D*], and AS160 [*E*]) (*$P < 0.05$ vs. control, †$P < 0.05$, ††$P < 0.01$ vs. Dex). In C2C12 cells stably overexpressing IRS1, Dex increases Ser[307] but does not induce Ser[24] phosphorylation (*F*). Ctrl, control. PMA, phorbol myristate acetate.

Mouse in vivo studies

Food intake, glucose tolerance, and insulin sensitivity. Food intake decreased within the first 48 h in the A2-treated animals in comparison with vehicle-treated controls. However, by day 4 and for the remainder of the 28-day protocol, food intake did not differ between the groups (day 4: 15.4 ± 0.7 vs. 16.5 ± 0.7 kcal/day [A2 vs. control], $P = 0.08$). At day 28, fasting blood glucose and insulin levels were lower in the A2-treated animals compared with both vehicle-treated and pair-fed controls (glucose: 6.8 ± 0.3 vs. 7.4 ± 0.35 vs. 7.7 ± 0.3 mmol/l, $P < 0.05$; insulin: 0.60 ± 0.10 vs. 0.82 ± 0.14 vs. 0.91 ± 0.11 ng/ml, $P < 0.05$, A2 vs. vehicle vs. pair-fed vehicle). Similarly, homeostasis model assessment values were lower (4.2 ± 0.9 vs. 6.0 ± 0.98 vs. 7.1 ± 0.9 [A2 vs. vehicle vs. pair-fed vehicle], $P < 0.05$) as was insulin secretion

(area under curve, AUC) across an OGTT (2.29 ± 0.23 vs. 2.95 ± 0.37 vs. 2.94 ± 0.21 ng·ml^{-1}·h^{-1} [A2 vs. vehicle vs. pair-fed vehicle], $P < 0.05$). Glucose levels across the OGTT (AUC) did not change significantly (22.4 ± 0.46 vs. 24.2 ± 0.42 vs. 22.9 ± 0.45 mmol·l^{-1}·h^{-1} [A2 vs. vehicle vs. pair-fed vehicle], $P =$ not significant).

Gene and protein expression in skeletal muscle from KK mice. Cortisone pellet–implanted KK mice treated with A2 for 4 consecutive days had increased total IRS1 protein expression, decreased Ser[307] phosphorylation, and increased Thr[308] phosphorylation of Akt/PKB in whole-tissue quadriceps explants. Tyr[608] phosphorylation did not change (Fig. 5*A*). Genecard analysis of quadriceps mRNA expression following A2 treatment is shown in Table 3. Positive findings were endorsed with real-time PCR (Fig. 5*B*). 11β-HSD1 expression decreased (0.48-fold) (Table 3,
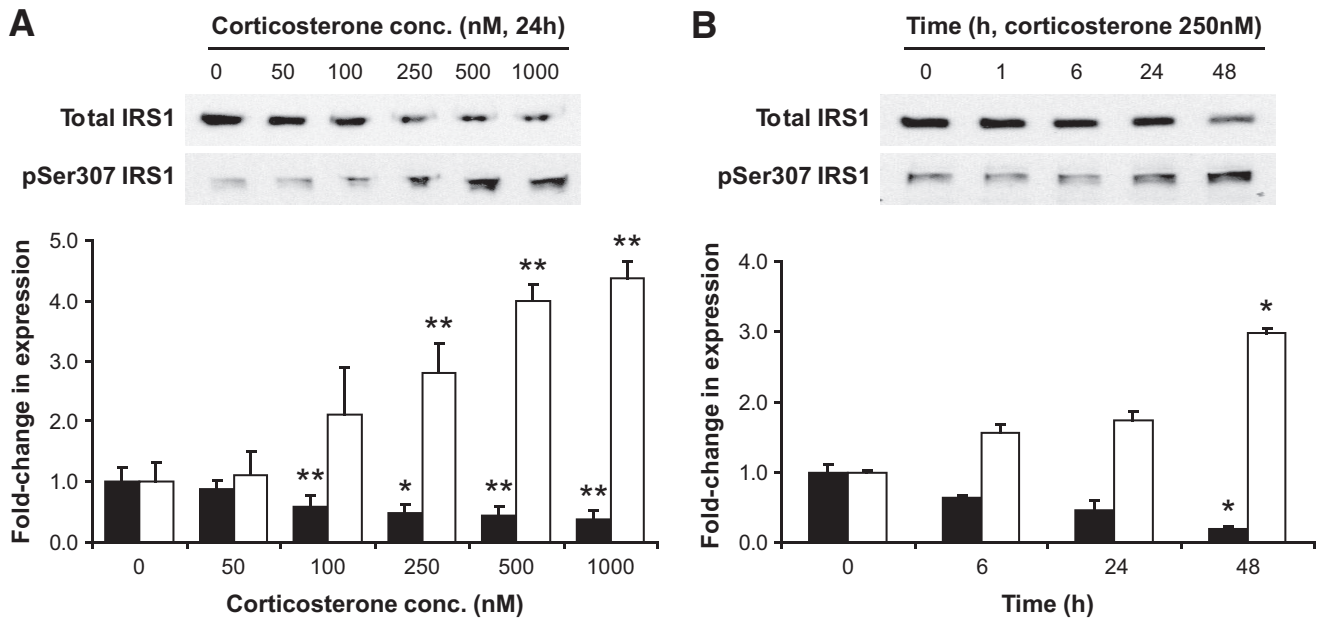
FIG. 2. The endogenous rodent glucocorticoid, CORT, induces a dose- (*A*) and time- (*B*) dependent decrease in total IRS1 protein expression (black bars) and increase in pSer[307] IRS1 (white bars). Data presented are the means of $n = 4$–6 experiments with representative Western blots inserted above (*$P < 0.05$, **$P < 0.01$ vs. control).

Fig. 5*B*) without effect on glucocorticoid receptor or H6PDH expression. In agreement with our protein expression data, IRS1 mRNA expression increased after selective 11β-HSD1 inhibition (Fig. 5*B*). The regulatory subunit of PI3K p85 decreased 0.25-fold after treatment with A2 with no change in catalytic subunit (p110) expression (Table 3, Fig. 5*B*). PI3K activity was not measured as part of this study. A2 treatment decreased expression of key target genes involved in lipogenesis (ACC1 0.3-fold, DGAT 0.4-fold), lipolysis (HSL 0.3-fold, ATGL 0.39-fold) and lipid oxidation (ACC2 0.6-fold) (Table 3, Fig. 5*B*). In addition, PDK4 increased 1.7-fold (Fig. 5*B*).

DISCUSSION

In this study, we have characterized in detail the impact of both synthetic and endogenous glucocorticoids upon insulin signaling in the rodent skeletal muscle cell line, C2C12. In addition, we have characterized expression and activity of 11β-HSD1 in both rodent and human skeletal muscle, ascribed a functional significance to its activity in terms of insulin sensitization, and have begun to explore the mechanisms by which this occurs.

Glucocorticoids impair insulin signaling at multiple levels, importantly decreasing total IRS1 protein expression and increasing Ser[307] phosphorylation. IRS-1 serine phosphorylation at this site has been reported to decrease the affinity of IRS1 for the insulin receptor and increased IRS1 degradation (9,10), and this may account for the decrease in total protein expression that we observed. It is also

sufficient to account for the glucocorticoid-induced decrease of insulin-stimulated glucose uptake. The pivotal role of IRS1 in skeletal muscle insulin signaling is highlighted by IRS1 knockout mice (22–24) that develop marked insulin resistance. Serine phosphorylation of IRS1 at numerous residues has been implicated in the development of insulin resistance (19,25–27). Specifically, Ser[307] phosphorylation is a negative regulator of IRS1 function. Inflammatory cytokines including tumor necrosis factor-α and C-reactive protein increase Ser[307] phosphorylation (28,29), and insulin itself has been described to have similar effects (30,31). Although several kinases have been implicated in serine phosphorylation of IRS1 (32), PKCθ is believed to have a critical role, notably after free fatty acid (FFA) exposure (33,34). PKCθ knockout animals resist lipid-induced skeletal muscle insulin resistance (35), and rodent models with muscle-specific targeted serine-to-alanine substitutions at residues within IRS1 including Ser[307] resist fat-induced insulin resistance (36). Glucocorticoid induction of lipolysis and consequent FFA generation (37) as well as increased FFA uptake will activate PKCθ, and this may well be an important contributor to the insulin resistance induced by glucocorticoid. This is endorsed by our gene expression analysis of lipogenic/lipolytyic genes in rodent muscle after 4-day treatment with the selective 11β-HSD1 inhibitor A2 (see discussion below). In addition, the lack of Ser[24] phosphorylation may also add weight to this hypothesis. PKCθ does not contribute to phorbol-12-myristate-13-acetate–induced

TABLE 2
Comparative mRNA expression of 11β-HSD1, glucocorticoid receptor, and H6PDH in mouse skeletal muscle and C2C12 myotubes

Gene	C2C12	Quadriceps	Liver	Adipose
11β-HSD1	32.9 ± 2.9	0.29 ± 0.03	18.40 ± 1.96	1.26 ± 0.14
H6PDH	0.10 ± 0.015	0.1 ± 0.006	0.12 ± 0.005	0.11 ± 0.0009
Glucocorticoid receptor	0.56 ± 0.022	5.67 ± 0.29	3.33 ± 0.36	3.9 ± 0.68

Data are expressed as AUs (AU means ± SE, $n = 3$–5 experiments). Expression in rodent liver and adipose tissue are provided as a quantitative reference.
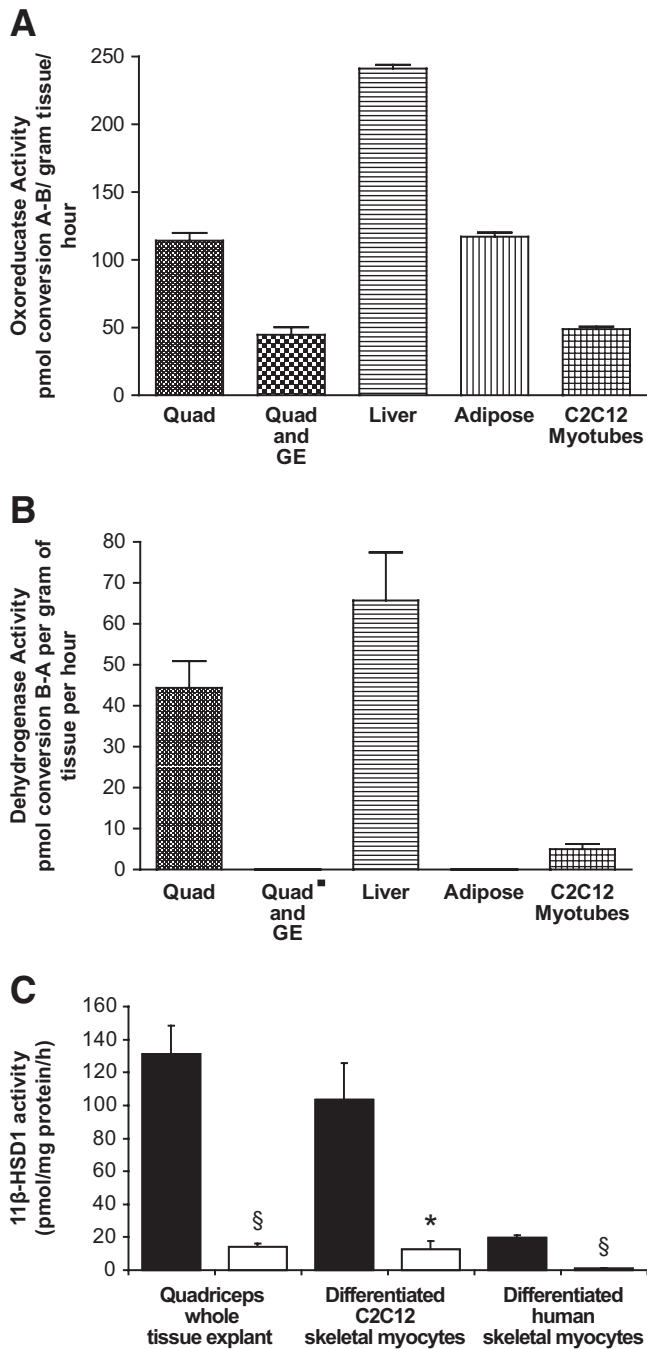
FIG. 3. Functional 11β-HSD1 enzyme oxo-reductase (A) and dehydrogenase (B) activity is present in explants of mouse quadriceps muscle with levels comparable with that seen in adipose tissue and liver. 11β-HSD1 activity is also observed in differentiated C2C12 rodent skeletal myocytes (data presented as picomole per milligram of protein per hour for C2C12 cells). Although dehydrogenase activity is present, the predominant activity is oxo-reductase generating active glucocorticoid. Coincubation of skeletal muscle explants with the nonselective 11β-HSD inhibitor, glycyrrhetinic acid, significantly decreases activity (data shown are the means ± SE of $n = 3$–6 experiments, *$P < 0.05$). In addition, the selective 11β-HSD1 inhibitor, A1 (1 μmol/l, 24 h), decreases oxo-reductase activity in rodent whole-tissue quadriceps explants, differentiated C2C12 skeletal myocytes, and primary cultures of human skeletal myocytes (C) (data shown are the means ± SE of $n = 3$–6 experiments, *$P < 0.05$, §$P < 0.005$) (control = black bars, A1 = white bars). GE, glycyrrhetinic acid.

Ser[24] phosphorylation but instead is dependent upon PKCα activation (19).

Other studies have also highlighted the pivotal role of IRS1 in glucocorticoid-associated insulin resistance, al-
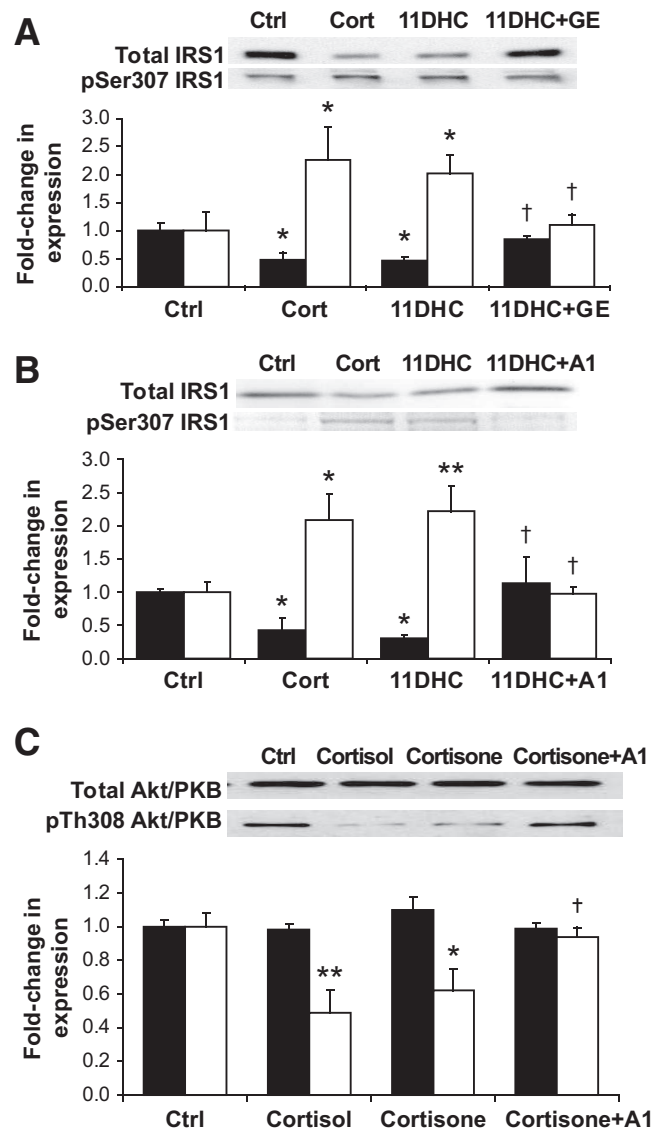

FIG. 4. Both CORT and 11DHC decrease IRS1 expression (black bars) and increase pSer[307] IRS1 (white bars). The activity of 11DHC is dependent upon its activation to CORT by 11β-HSD1. Inhibition of 11β-HSD1 using glycyrrhetinic acid (A) or the selective 11β-HSD1 inhibitor, A1 (B), reverses the effect of 11DHC upon IRS1 expression and phosphorylation. Similarly, in primary cultures of human myotubes, A1 blocks the cortisone-induced decrease in pThr[308] Akt/PKB (white bars) after insulin stimulation without changing total Akt/PKB expression (black bars) (C). Data presented are the mean of $n = 4$ experiments with representative Western blots inserted (*$P < 0.05$, **$P < 0.01$ vs. control, †$P < 0.05$ vs. 11DHC or cortisone). Ctrl, control.

though serine phosphorylation has not been examined. The results of these studies do show a degree of variability and some but not all have shown decreased activating tyrosine phosphorylation of IRS1 (11–13). Others have reported changes in insulin receptor expression and activation, PI3K activity and expression, and IRS2 expression and phosphorylation (12,38,39). The explanation for these inconsistencies is not entirely clear but may reflect differences between animal and cell models and specific investigative protocols.

Downstream of IRS1, we observed decreased activating pSer[473] Akt/PKB and pThr[308] Akt/PKB, and we propose that this may be a direct consequence of reduced insulin signaling capacity through enhanced IRS1 inactivation. In addition, we observed an increase in AS160 protein ex-
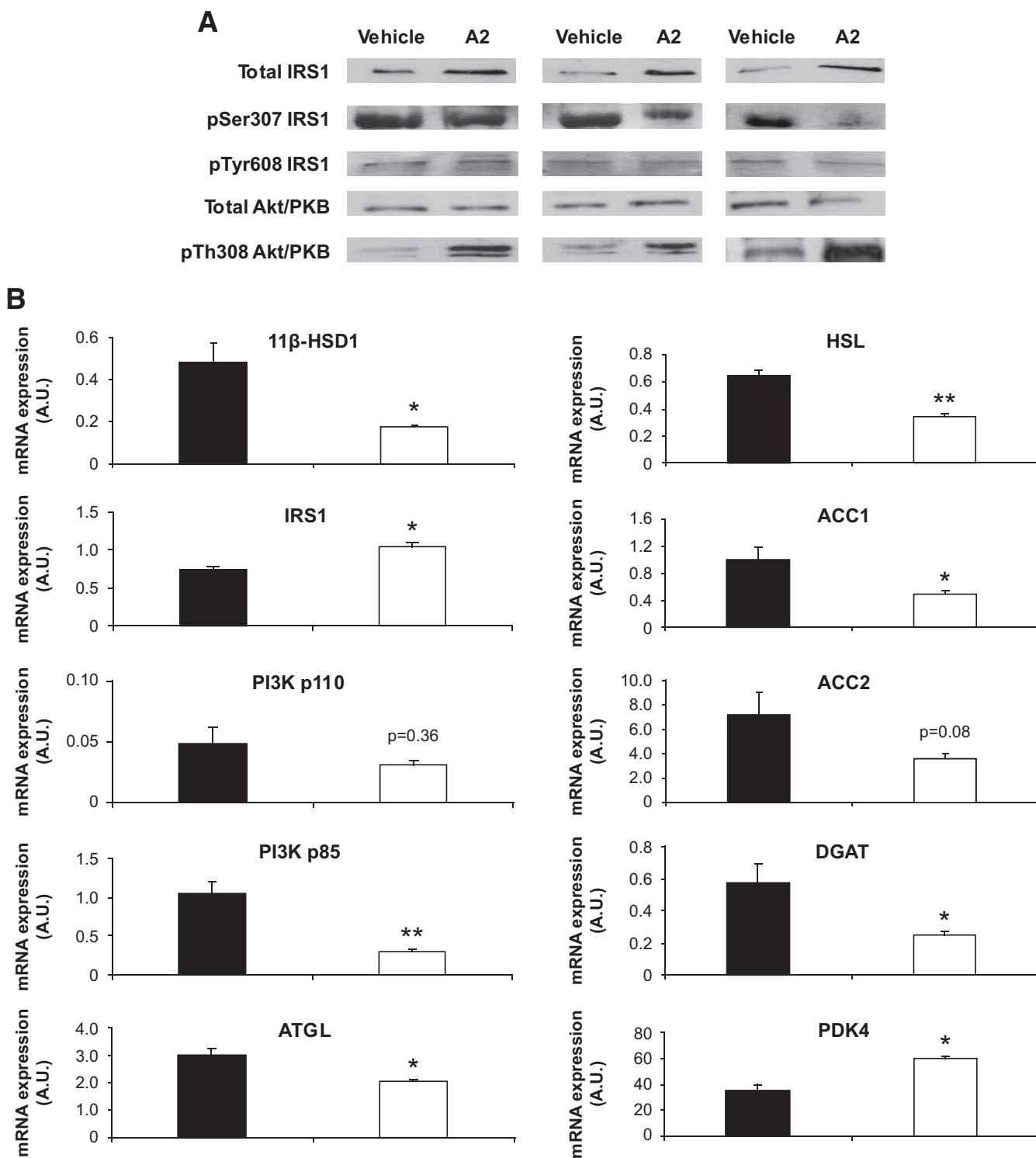
FIG. 5. In cortisone pellet–implanted KK mice, the selective 11β-HSD1 inhibitor, A2, increases IRS1 total protein expression, decreases inactivating pSer^{307} IRS1, and further downstream enhances insulin-stimulated pThr^{308} Akt/PKB in quadriceps muscle explants. Representative Western blots are shown (A2 vs. vehicle) (*A*). Real-time PCR analysis endorsing observation from the Genecard analysis presented in Table 3. Gene expression from whole-tissue quadriceps explants obtained from cortisone pellet–implanted KK mice treated for 4 days with the selective 11β-HSD1 inhibitor, A2 (white bars), or vehicle (black bars) (*$P < 0.05$, **$P < 0.01$) ($n = 3$ per group) (*B*).

pression. AS160 is a recently identified protein with Rab-guanosine triphosphate (GTP)ase activity. Under basal conditions, it is resident within GLUT4-containing vesicles and limits the GTP availability that is necessary for vesicle translocation to the cell membrane to permit glucose entry. Upon phosphorylation by activated Akt/PKB, AS160 dissociates from the vesicle, allowing GTP to bind to Rab

proteins and vesicle translocation to the cell membrane to occur (7). While regulation of AS160 phosphorylation at differing sites by growth factors including IGF-1 and EGF has been described (40), glucocorticoid regulation has not been explored. Our data show that glucocorticoids increase both AS160 protein and mRNA expression in a glucocorticoid receptor–dependent mechanism. These ob-

TABLE 3

Quadriceps skeletal muscle Genecard analysis of 45 preselected gene targets implicated in the pathogenesis of glucocorticoid-induced insulin resistance

	Gene of interest	Cortisone + vehicle (means Δct ± SE)	Cortisone + A2 (means Δct ± SE)	Fold change in gene expression after M1 treatment
	Insr	15.9 ± 0.2	16.5 ± 0.2	0.65
	Irs1	16.9 ± 0.1	16.6 ± 0.1	1.27
	Irs2	17.2 ± 0.2	16.3 ± 0.8	1.93
	Pik3r1 (p85α)	14.9 ± 0.2	16.9 ± 0.4	**0.25**
	Pik3cb (p110β)	19.4 ± 0.3	19.8 ± 0.1	0.79
	Pdk1	15.9 ± 0.2	16.9 ± 0.1	**0.49**
	Akt1	16.3 ± 0.1	17.1 ± 0.2	0.59
	Akt2	17.7 ± 0.3	18.2 ± 0.3	0.74
	Prkcz (PKCζ)	19.2 ± 0.3	20.6 ± 0.6	**0.37**
	Prkci (PKCλ)	19.6 ± 0.1	20.2 ± 0.1	0.62
	Tbc1d1	15.7 ± 0.3	16.5 ± 0.1	0.58
	Tbc1d4 (AS160)	17.2 ± 0.3	18.1 ± 0.3	0.53
	Rab10	11.7 ± 0.3	12.3 ± 0.1	0.68
	Slc2a1 (GLUT-1)	16.8 ± 0.2	17.0 ± 0.1	0.91
	Slc2a4 (GLUT-4)	14.1 ± 0.1	14.1 ± 0.1	1.03
	Ptpn1 (PTP-1b)	17.8 ± 0.1	18.8 ± 0.1	0.52
	Ptpn11 (SHP2)	16.1 ± 0.2	16.4 ± 0.1	0.77
	Pten	15.8 ± 0.1	16.6 ± 0.1	0.60
	Ppp2r1a (PP2A)	14.9 ± 0.2	15.2 ± 0.1	0.81
	Socs1	21.5 ± 0.4	21.2 ± 0.4	1.20
	Socs3	19.4 ± 0.2	19.4 ± 0.1	0.98
	Frap1 (mTOR)	16.5 ± 0.2	17.3 ± 0.3	0.55
	Foxo1	16.9 ± 0.2	17.4 ± 0.1	0.75
	Foxo3a	15.9 ± 0.1	16.7 ± 0.5	0.58
	Prkaa2 (AMPK)	14.8 ± 0.1	15.0 ± 0.3	0.91
Insulin signalling cascade	Ppargc1a (PGC-1α)	16.9 ± 0.2	17.1 ± 0.1	0.93
	H6pd	15.6 ± 0.1	16.2 ± 0.3	0.66
Glucocorticoid	Hsd11b1 (11β-HSD1)	17.5 ± 0.6	18.5 ± 0.8	**0.48**
metabolism and action	Nr3c1 (GRα)	15.8 ± 0.1	16.3 ± 0.2	0.72
	Acaca (ACC1)	15.1 ± 1.0	16.7 ± 0.2	**0.33**
	Acacb (ACC2)	13.6 ± 0.3	14.4 ± 0.2	0.60
	Lpl	12.6 ± 0.2	13.2 ± 0.1	0.68
	Lipe (HSL)	16.4 ± 0.6	18.1 ± 0.1	**0.30**
	Pnpla2 (ATGL)	13.7 ± 0.5	15.1 ± 0.1	**0.39**
	Dgkd (DGKδ)	21.3 ± 0.5	21.4 ± 0.1	0.97
Lipid metabolism	Pparg (PPARγ)	21.2 ± 0.5	22.4 ± 0.3	**0.43**
	Sptlc1 (SPT1)	17.8 ± 0.1	18.6 ± 0.0	0.59
	Ugcg (glucosylceramide synthase)	18.8 ± 0.1	19.5 ± 0.1	0.61
	Asah1 (acid ceramidase)	19.0 ± 0.1	19.3 ± 0.1	0.82
	Lass1	16.9 ± 0.1	17.3 ± 0.1	0.77
Ceramide metabolism	Lass6	20.5 ± 0.4	21.1 ± 0.0	0.68
	Prkca (PKC-α)	16.6 ± 0.2	16.6 ± 0.1	0.94
	Prkcb1 (PKC-β)	22.7 ± 0.3	22.8 ± 0.3	0.96
	Prkcc PKC-γ)	22.6 ± 0.1	23.1 ± 0.7	0.69
Other genes	Ppara (PPARα)	18.7 ± 0.3	19.0 ± 0.1	0.85
	Ppib (cyclophilin B)	18.1 ± 0.2	18.4 ± 0.1	0.79
Internal controls	Hprt1	16.5 ± 0.2	17.1 ± 0.0	0.69

Cortisone pellet–implanted KK mice were treated with a selective 11β-HSD1 inhibitor, A2, or vehicle for 4 days before animals were killed ($n = 3$ per group, for detailed protocol see RESEARCH DESIGNS AND METHODS). Data presented as means Δct ± SE for both groups of animals relative to 18 s as an internal housekeeping gene, higher Δct values corresponding with lower gene expression. Fold changes in gene expression were calculated as described in RESEARCH DESIGNS AND METHODS. Specific target genes and all changes >2-fold increase or 0.5-fold decrease vs. vehicle (highlighted in bold) were endorsed with real-time PCR (see Fig. 5).

servations are interesting and point toward a separate mechanism of regulation rather than simply a downstream consequence of decreased IRS1 activation.

Although the net effect of glucocorticoid was to induce insulin resistance, we did observe an increase in IRS2 mRNA and protein expression. In addition IR, PI3K (p85 subunit), and GLUT4 mRNA expression increased, although protein expression was not examined in this study nor was PI3K-specific activity. It is possible that this represents a compensatory mechanism to preserve insulin sensitivity in an attempt to compensate for the inhibition of signaling through IRS1. However, overall the effect of

glucocorticoid exposure is to limit insulin-stimulated glucose uptake.

In addition to the effect of exogenous glucocorticoids, we have shown that prereceptor metabolism of endogenous glucocorticoid by 11β-HSD1 is a crucial regulator of insulin sensitivity in skeletal muscle. 11β-HSD1 is expressed and biologically active in human skeletal muscle (41). Overexpression of 11β-HSD1 has been described in rodent skeletal muscle in models of diabetes (42) and myotubes isolated from patients with insulin resistance and type 2 diabetes (43,44). However, this is not a consistent finding (45), and its precise contribution to metabolic and muscle phenotype is still to be clarified. Selective 11β-HSD1 inhibitors are currently in development; in rodents and primates they limit local glucocorticoid availability and improve glucose tolerance, lipid profiles, and insulin sensitivity (16,46). Very recently, studies using in vitro differentiated primary in human myoblasts have shown that 11β-HSD1 inhibition (pharmacological or siRNA) can limit cortisone- but not cortisol-induced changes in glucose uptake, glycogen synthesis, and palmitate oxidation. However, in this model, an insulin-sensitizing action could not be demonstrated (47). In our study, we have clearly shown expression and activity of 11β-HSD1 in human and rodent skeletal muscle that is blocked by selective and nonselective 11β-HSD1 inhibitors. This is functionally important and not only restores IRS1 protein levels to control values but also decreases pSer^{307} IRS1, enhances Akt/PKB activation, and may represent an important insulin-sensitizing mechanism of selective 11β-HSD1 inhibitors. These observations appear consistent in both our in vitro and rodent in vivo models. A2 has an insulin-sensitizing action as evidenced by decreased fasting glucose and insulin levels, decreased homeostasis model assessment scores, and reduced insulin secretion across an OGTT. Unfortunately, clamp studies were not performed as part of this protocol but have been reported elsewhere with other selective 11β-HSD1 inhibitors (16). In addition to the actions described above, A2 administration to mice in vivo decreased lipogenic gene expression (ACC1, FAS, and DGAT) and increased FFA utilization (decreased ACC2 leading to a decrease in the malonyl CoA-mediated inhibition of β-oxidation) in agreement with published observations (48). Furthermore, decreased HSL and ATGL will afford decreases in FFA and DAG generation. Interestingly, we also observed a 1.7-fold increase in PDK4 expression with A2 treatment in vivo. PDK4 is a negative regulator of the pyruvate dehydrogenase complex, limiting acetyl CoA generation. Rodents with deletion of PDK4 have increased glucose oxidation (49), and in cell culture systems, glucocorticoids increase PDK4 expression (47). The discrepancies with our data, where A2 increased PDK4 expression, almost certainly reflect the complexities of whole-animal versus cell culture models (we too have observed decreased PDK4 expression after Dex treatment in C2C12 myotubes [data not shown]). Importantly, the increase in PDK4 with selective 11β-HSD1 inhibitors may further serve to drive lipid oxidation at the expense of glucose oxidation. The net effect of all these observations will be to decrease intramyocellular lipid accumulation as well as local FFA and DAG generation. Consequently, PKCθ activation will be decreased, and this may be responsible for the reduction in Ser^{307} phosphorylation after selective 11β-HSD1 inhibition. However, this hypothesis remains to be proven and needs to be addressed in future studies.

In conclusion, Ser^{307} phosphorylation of IRS1 is a novel mechanism of glucocorticoid-induced insulin resistance. The prereceptor modulation of glucocorticoid availability is an important regulator of glucocorticoid action in skeletal muscle. Selective 11β-HSD1 inhibitors enhance insulin action, and we propose that this may predominantly be through modulation of lipid metabolism within skeletal muscle. Clinical data utilizing 11β-HSD1 inhibitors are beginning to emerge in obese patients and those with type 2 diabetes (50); it is likely that their efficacy in muscle will provide an additional pharmacological benefit in the treatment of type 2 diabetes and insulin resistance.

REFERENCES

1. Van Staa TP, Leufkens HG, Abenhaim L, Begaud B, Zhang B, Cooper C. Use of oral corticosteroids in the United Kingdom. Q J Med 2000;93:105–111
2. Larsson H, Ahren B. Short-term dexamethasone treatment increases plasma leptin independently of changes in insulin sensitivity in healthy women. J Clin Endocrinol Metab 1996;81:4428–4432
3. Fraser R, Ingram MC, Anderson NH, Morrison C, Davies E, Connell JM. Cortisol effects on body mass, blood pressure, and cholesterol in the general population. Hypertension 1999;33:1364–1368
4. Tomlinson JW, Walker EA, Bujalska IJ, Draper N, Lavery GG, Cooper MS, Hewison M, Stewart PM. 11β-hydroxysteroid dehydrogenase type 1: a tissue-specific regulator of glucocorticoid response. Endocr Rev 2004;25:831–866
5. Lavery GG, Walker EA, Draper N, Jeyasuria P, Marcos J, Shackleton CH, Parker KL, White PC, Stewart PM. Hexose-6-phosphate dehydrogenase knockout mice lack 11β-hydroxysteroid dehydrogenase type 1-mediated glucocorticoid generation. J Biol Chem 2006;281:6546–6551
6. Hanada M, Feng J, Hemmings BA. Structure, regulation and function of PKB/AKT: major therapeutic target. Biochim Biophys Acta 2004;1697:3–16
7. Sano H, Kane S, Sano E, Miinea CP, Asara JM, Lane WS, Garner CW, Lienhard GE. Insulin-stimulated phosphorylation of a Rab GT. Pase-activating protein regulates GLUT4 translocation. J Biol Chem 2003;278:14599–14602
8. Watson RT, Kanzaki M, Pessin JE. Regulated membrane trafficking of the insulin-responsive glucose transporter 4 in adipocytes. Endocr Rev 2004;25:177–204
9. Aguirre V, Uchida T, Yenush L, Davis R, White MF. The c-Jun NH(2)-terminal kinase promotes insulin resistance during association with insulin receptor substrate-1 and phosphorylation of Ser(307). J Biol Chem 2000;275:9047–9054
10. Aguirre V, Werner ED, Giraud J, Lee YH, Shoelson SE, White MF. Phosphorylation of Ser307 in insulin receptor substrate-1 blocks interactions with the insulin receptor and inhibits insulin action. J Biol Chem 2002;277:1531–1537
11. Giorgino F, Almahfouz A, Goodyear LJ, Smith RJ. Glucocorticoid regulation of insulin receptor and substrate IRS-1 tyrosine phosphorylation in rat skeletal muscle in vivo. J Clin Invest 1993;91:2020–2030
12. Rojas FA, Hirata AE, Saad MJ. Regulation of insulin receptor substrate-2 tyrosine phosphorylation in animal models of insulin resistance. Endocrine 2003;21:115–122
13. Saad MJ, Folli F, Kahn JA, Kahn CR. Modulation of insulin receptor, insulin

receptor substrate-1, and phosphatidylinositol 3-kinase in liver and muscle of dexamethasone-treated rats. J Clin Invest 1993;92:2065–2072

14. Ruzzin J, Wagman AS, Jensen J. Glucocorticoid-induced insulin resistance in skeletal muscles: defects in insulin signalling and the effects of a selective glycogen syntheses kinase-3 inhibitor. Diabetologia 2005;48:2119–2130

15. Morton NM, Holmes MC, Fievet C, Staels B, Tailleux A, Mullins JJ, Seckl JR. Improved lipid and lipoprotein profile, hepatic insulin sensitivity, and glucose tolerance in 11β-hydroxysteroid dehydrogenase type 1 null mice. J Biol Chem 2001;276:41293–41300

16. Alberts P, Nilsson C, Selen G, Engblom LO, Edling NH, Norling S, Klingstrom G, Larsson C, Forsgren M, Ashkzari M, Nilsson CE, Fiedler M, Bergqvist E, Eva BB, Abrahmsen LB. Selective inhibition of 11{β}-hydroxysteroid dehydrogenase type 1 improves hepatic insulin sensitivity in hyperglycemic mice strains. Endocrinology 2003;144:4755–4762

17. Berthiaume M, Laplante M, Festuccia W, Gelinas Y, Poulin S, Lalonde J, Joanisse DR, Thieringer R, Deshaies Y. Depot-specific modulation of rat intraabdominal adipose tissue lipid metabolism by pharmacological inhibition of 11β-hydroxysteroid dehydrogenase type 1. Endocrinology 2007;148:2391–2397

18. Hermanowski-Vosatka A, Balkovec JM, Cheng K, Chen HY, Hernandez M, Koo GC, Le Grand CB, Li Z, Metzger JM, Mundt SS, Noonan H, Nunes CN, Olson SH, Pikounis B, Ren N, Robertson N, Schaeffer JM, Shah K, Springer MS, Strack AM, Strowski M, Wu K, Wu T, Xiao J, Zhang BB, Wright SD, Thieringer R. 11β-HSD1 inhibition ameliorates metabolic syndrome and prevents progression of atherosclerosis in mice. J Exp Med 2005;202:517–527

19. Nawaratne R, Gray A, Jorgensen CH, Downes CP, Siddle K, Sethi JK. Regulation of insulin receptor substrate 1 pleckstrin homology domain by protein kinase C: role of serine 24 phosphorylation. Mol Endocrinol 2006;20:1838–1852

20. Tomlinson JW, Finney J, Gay C, Hughes BA, Hughes SV, Stewart PM. Impaired glucose tolerance and insulin resistance are associated with increased adipose 11β-hydroxysteroid dehydrogenase type 1 expression and elevated hepatic 5α-reductase activity. Diabetes 2008;57:2652–2660

21. Liu F, Kim J, Li Y, Liu X, Li J, Chen X. An extract of Lagerstroemia speciosa L. has insulin-like glucose uptake-stimulatory and adipocyte differentiation-inhibitory activities in 3T3–L1 cells. J Nutr 2001;131:2242–2247

22. Araki E, Lipes MA, Patti ME, Bruning JC, Haag B III, Johnson RS, Kahn CR. Alternative pathway of insulin signalling in mice with targeted disruption of the IRS-1 gene. Nature 1994;372:186–190

23. Kido Y, Burks DJ, Withers D, Bruning JC, Kahn CR, White MF, Accili D. Tissue-specific insulin resistance in mice with mutations in the insulin receptor, IRS-1, and IRS-2. J Clin Invest 2000;105:199–205

24. Previs SF, Withers DJ, Ren JM, White MF, Shulman GI. Contrasting effects of IRS-1 versus IRS-2 gene disruption on carbohydrate and lipid metabolism in vivo. J Biol Chem 2000;275:38990–38994

25. Mussig K, Fiedler H, Staiger H, Weigert C, Lehmann R, Schleicher ED, Haring HU. Insulin-induced stimulation of JNK and the PI 3-kinase/mTOR pathway leads to phosphorylation of serine 318 of IRS-1 in C2C12 myotubes. Biochem Biophys Res Commun 2005;335:819–825

26. Werner ED, Lee J, Hansen L, Yuan M, Shoelson SE. Insulin resistance due to phosphorylation of insulin receptor substrate-1 at serine 302. J Biol Chem 2004;279:35298–35305

27. Waraich RS, Weigert C, Kalbacher H, Hennige AM, Lutz SZ, Haring HU, Schleicher ED, Voelter W, Lehmann R. Phosphorylation of Ser357 of rat insulin receptor substrate-1 mediates adverse effects of protein kinase C-delta on insulin action in skeletal muscle cells. J Biol Chem 2008;283:11226–11233

28. D'Alessandris C, Lauro R, Presta I, Sesti G. C-reactive protein induces phosphorylation of insulin receptor substrate-1 on Ser307 and Ser 612 in L6 myocytes, thereby impairing the insulin signalling pathway that promotes glucose transport. Diabetologia 2007;50:840–849

29. de AC, Teruel T, Hernandez R, Lorenzo M. Tumor necrosis factor-α produces insulin resistance in skeletal muscle by activation of inhibitor κB kinase in a p38 MAPK-dependent manner. J Biol Chem 2004;279:17070–17078

30. Gual P, Gremeaux T, Gonzalez T, Le Marchand-Brustel Y, Tanti JF. MAP kinases and mTOR mediate insulin-induced phosphorylation of insulin receptor substrate-1 on serine residues 307, 612 and 632. Diabetologia 2003;46:1532–1542

31. Danielsson A, Nystrom FH, Stralfors P. Phosphorylation of IRS1 at serine 307 and serine 312 in response to insulin in human adipocytes. Biochem Biophys Res Commun 2006;342:1183–1187

32. Draznin B. Molecular mechanisms of insulin resistance: serine phosphorylation of insulin receptor substrate-1 and increased expression of p85α: the two sides of a coin. Diabetes 2006;55:2392–2397

33. Yu C, Chen Y, Cline GW, Zhang D, Zong H, Wang Y, Bergeron R, Kim JK, Cushman SW, Cooney GJ, Atcheson B, White MF, Kraegen EW, Shulman GI. Mechanism by which fatty acids inhibit insulin activation of insulin receptor substrate-1 (IRS-1)-associated phosphatidylinositol 3-kinase activity in muscle. J Biol Chem 2002;277:50230–50236

34. Gao Z, Zhang X, Zuberi A, Hwang D, Quon MJ, Lefevre M, Ye J. Inhibition of insulin sensitivity by free fatty acids requires activation of multiple serine kinases in 3T3–L1 adipocytes. Mol Endocrinol 2004;18:2024–2034

35. Kim JK, Fillmore JJ, Sunshine MJ, Albrecht B, Higashimori T, Kim DW, Liu ZX, Soos TJ, Cline GW, O'Brien WR, Littman DR, Shulman GI. PKC-θ knockout mice are protected from fat-induced insulin resistance. J Clin Invest 2004;114:823–827

36. Morino K, Neschen S, Bilz S, Sono S, Tsirigotis D, Reznick RM, Moore I, Nagai Y, Samuel V, Sebastian D, White M, Philbrick W, Shulman GI. Muscle-specific IRS-1 Ser→Ala transgenic mice are protected from fat-induced insulin resistance in skeletal muscle. Diabetes 2008;57:2644–2651

37. Djurhuus CB, Gravholt CH, Nielsen S, Mengel A, Christiansen JS, Schmitz OE, Moller N. Effects of cortisol on lipolysis and regional interstitial glycerol levels in humans. Am J Physiol Endocrinol Metab 2002;283:E172–E177

38. Giorgino F, Pedrini MT, Matera L, Smith RJ. Specific increase in p85α expression in response to dexamethasone is associated with inhibition of insulin-like growth factor-I stimulated phosphatidylinositol 3-kinase activity in cultured muscle cells. J Biol Chem 1997;272:7455–7463

39. Giorgino F, Smith RJ. Dexamethasone enhances insulin-like growth factor-I effects on skeletal muscle cell proliferation. Role of specific intracellular signaling pathways. J Clin Invest 1995;96:1473–1483

40. Geraghty KM, Chen S, Harthill JE, Ibrahim AF, Toth R, Morrice NA, Vandermoere F, Moorhead GB, Hardie DG, MacKintosh C. Regulation of multisite phosphorylation and 14–3-3 binding of AS160 in response to IGF-1, EGF, PMA and AICAR. Biochem J 2007;407:231–241

41. Jang C, Obeyesekere VR, Dilley RJ, Alford FP, Inder WJ. 11Beta hydroxysteroid dehydrogenase type 1 is expressed and is biologically active in human skeletal muscle. Clin Endocrinol (Oxf) 2006;65:800–805

42. Zhang M, Lv XY, Li J, Xu ZG, Chen L. Alteration of 11β-hydroxysteroid dehydrogenase type 1 in skeletal muscle in a rat model of type 2 diabetes. Mol Cell Biochem 2009;324:147–155

43. Abdallah BM, Beck-Nielsen H, Gaster M. Increased expression of 11β-hydroxysteroid dehydrogenase type 1 in type 2 diabetic myotubes. Eur J Clin Invest 2005;35:627–634

44. Whorwood CB, Donovan SJ, Flanagan D, Phillips DI, Byrne CD. Increased glucocorticoid receptor expression in human skeletal muscle cells may contribute to the pathogenesis of the metabolic syndrome. Diabetes 2002;51:1066–1075

45. Jang C, Obeyesekere VR, Dilley RJ, Krozowski Z, Inder WJ, Alford FP. Altered activity of 11β-hydroxysteroid dehydrogenase types 1 and 2 in skeletal muscle confers metabolic protection in subjects with type 2 diabetes. J Clin Endocrinol Metab 2007;92:3314–3320

46. Bhat BG, Hosea N, Fanjul A, Herrera J, Chapman J, Thalacker F, Stewart PM, Rejto P. Demonstration of proof of mechanism and pharmacokinetics and pharmacodynamic relationship with PF-915275, an inhibitor of 11{β}HSD1, in cynomolgus monkeys. J Pharmacol Exp Ther 2007;324:299–305

47. Salehzadeh F, Al-Khalili L, Kulkarni SS, Wang M, Lonnqvist F, Krook A. Glucocorticoid-mediated effects on metabolism are reversed by targeting 11β hydroxysteroid dehydrogenase type 1 in human skeletal muscle. Diabete Metab Res Rev 2009;25:250–258

48. Berthiaume M, Laplante M, Festuccia WT, Cianflone K, Turcotte LP, Joanisse DR, Olivecrona G, Thieringer R, Deshaies Y. 11β-HSD1 inhibition improves triglyceridemia through reduced liver VLDL secretion and partitions lipids toward oxidative tissues. Am J Physiol Endocrinol Metab 2007;293:E1045–E1052

49. Jeoung NH, Harris RA. Pyruvate dehydrogenase kinase-4 deficiency lowers blood glucose and improves glucose tolerance in diet-induced obese mice. Am J Physiol Endocrinol Metab 2008;295:E46–E54

50. Hawkins M, Hunter D, Kishore P, Schwartz S, Hompesch M, Hollis G, Levy R, Williams B, Huber R. INCB013739, a Selective Inhibitor of 11β-Hydroxysteroid Dehydrogenase Type 1 (11βHSD1), Improves Insulin Sensitivity and Lower Plasma Cholesterol Over 28 Days in Patients with Type 2 Diabetes Mellitus (Abstract). 68th Scientific Sessions of the American Diabetes Association, 6–10 June 2008, Moscone Convention Center, San Francisco, California